(G-cubed]

Supporting Information for

Magnetic fingerprints of modern sediments in the South China Sea resulting from source-to-sink processes.

Kissel, C.[1], Sarnthein, M.[2], Laj, C.[3], Wang, P.[4], Wandres, C.[1], Egli, R.[5]

[1] Laboratoire des Sciences du Climat et de l'Environnement/IPSL, CEA-CNRS-UVSQ, Université Paris-Saclay, 91198 Gif-sur-Yvette Cédex, France (Catherine.kissel@lsce.ipsl.fr)
[2] Institute of Geosciences, University of Kiel, Olshausenstr. 40, 24098 Kiel, Germany
[3] Ecole Normale Supérieure, PSL Research University, Département de Géosciences, 24 rue Lhomond, 75231 Paris Cédex 5, France.
[4] State Key Laboratory of Marine Geology, Tongji University, 1239 Siping Road, 200092 Shanghai, China
[5] Central Institute for Meteorology and Geodynamics, Department of Geophysics, 1190 Vienna, Hohe Warte 38, Austria.

** corresponding author*
E-mail address: Catherine.Kissel@lsce.ipsl.fr

Contents of this file :

Text S1
Figure S1
Table S1

Introduction

The supporting information reported here provides the description of the laboratory procedures used to obtained the data discussed in the article. It also contains one figure showing the detailed result of the interpretation of the FORC diagram using the VARIFORC software. Finally, a table in .xlsx format contains all the numerical data discussed in the article and reported in the figures.

Text S1: Laboratory methods

The low-field magnetic susceptibility was measured with a MS2B Bartington sensor. The measurements were made over a 10 seconds integration time. The mass susceptibility (χ) was obtained by dividing volume magnetic susceptibility by the density of the sample.

The anhysteretic remanent magnetization (ARM) was imparted to the same samples using a 50 μT direct current (DC) field superimposed to a 100 mT alternating field (AF). The susceptibility of ARM (χ_{ARM}) was calculated as the DC field-normalized ARM. The ARM was stepwise demagnetized up to 80 mT in 10 successive steps (5, 10, 15, 20, 25, 30, 35, 40, 60, 80 mT) using an AGICO LDA-3A-demagnetizer with a tumbling sample holder. Finally, the median destructive field of ARM (MDF_{ARM}) and the percentage of magnetization remaining after demagnetization at 80 mT with respect to the initial value ($\%ARM_{80mT} = 100 \times ARM_{80mT}/ARM_{0mT}$) were calculated.

Subsequently, the isothermal remanent magnetization (IRM) was stepwise acquired on the same samples with 6 successive steps up to 1 T using an Applied Physics pulse magnetizer. This IRM_{1T} then was stepwise AF demagnetized using the same steps as for the ARM. In the same way as for ARM, MDF_{IRM} and $\%IRM_{80mT}$ were determined. The S-ratio was calculated after applying a 0.3 T backfield ($IRM_{-0.3\,T}$) to the IRM_{1T} and using the definition ($= -IRM_{-0.3\,T}/IRM_{1T}$) of King and Channell (1991).

The hysteresis loops were performed on a few milligrams of dry sediment using an AGM (Micromag 2900) between +1 and -1 T (150 milliseconds averaging time). Saturation magnetization (M_s), remanent saturation magnetization (M_{rs}), and coercive force (B_c) were determined after high field slope correction calculated on the 0.7 to 1T interval. The remanent coercive force (B_{cr}) and S-ratio were determined by applying increasing back-fields after saturation at 1 T. The S-ratio derived from the hysteresis measurements made on dry samples were similar to those obtained on the wet cubic samples indicating that no change occurred in the magnetic mineralogy upon drying. High-resolution IRM acquisition curves were decomposed into cumulative log Gaussian (CLG) curves (Robertson & France, 1994) using the software proposed by Kruiver et al. (2001). The different coercitive families ($CLG_{\#}$) are defined by their half saturation IRM field ($B_{1/2}$), the percentage of their contribution to the total IRM and their dispersion parameter (DP) after minimizing the sum of squared residuals.

The thermal behavior of the samples was characterized with stepwise thermal demagnetizations of 3-axes IRM between room temperature and 650°C - 690°C (Lowrie, 1990). Samples with cubic shapes were first dried and fields of 1 T, 0.3 T, and 0.1 T were successively applied, each along one axis of the cubes, using an Applied Physics pulse magnetizer. The samples then were demagnetized using a zero-field PYROX furnace keeping the temperature gradient lower than 3-4°C at high temperatures over the interval in which the samples are placed. After heating, the samples were pushed into an air-cooled chamber where the residual field was < 2 nT.

All remanent magnetizations (IRM, ARM, 3-axes IRM) were measured using a 2G-755R cryogenic magnetometer (sensitivity 10^{-11} Am^2) equipped with high-homogeneity pick-up coils and placed together with the zero-field furnace and the AGICO LDA-3A AF demagnetizer within the μmetal shielded room at LSCE.

High-resolution FORC measurements (field increments: 0.5 mT) have been performed with an AGM (Micromag 2900) and processed with the VARIFORC software (Egli, 2013) to obtain the FORC diagram and the coercivity distributions corresponding to DC demagnetization curve contained in the FORC protocol and to the central ridge of the FORC diagram.

Egli, R. (2013). VARIFORC: An optimized protocol for the calculation of non-regular first-order reversal curve (FORC) diagrams. *Global and Planetary Change*. https://doi.org/ 10.1016/j.gloplacha.2013.08.003.

King, J., & Channell, J.E.T. (1991). Sedimentary magnetism, environmental magnetism, and magnetostratigraphy. In *U.S. National Report to International Union Geodesy and Geophysics, Review of Geophysics Supplement,* 29, 358–370.

Kruiver, P.P., Dekkers, M.J., & Heslop, D. (2001). Quantification of magnetic coercivity components by the analysis of acquisition curves of isothermal remanent magnetisation. *Earth and Planetary Science Letters*, 189, 269–276.

Lowrie, W. (1990). Identification of ferromagnetic minerals in a rock by coercivity and unblocking temperature properties. *Geophysical Research Letters,* 17, 159–162.

Robertson D.J., & France, D.E. (1994). Discrimination of remanence-carrying minerals in mixtures, using isothermal remanent magnetisation acquisition curves. *Physics of the Earth and Planetary Interiors*, 82, 223–234.

Figure S1 :

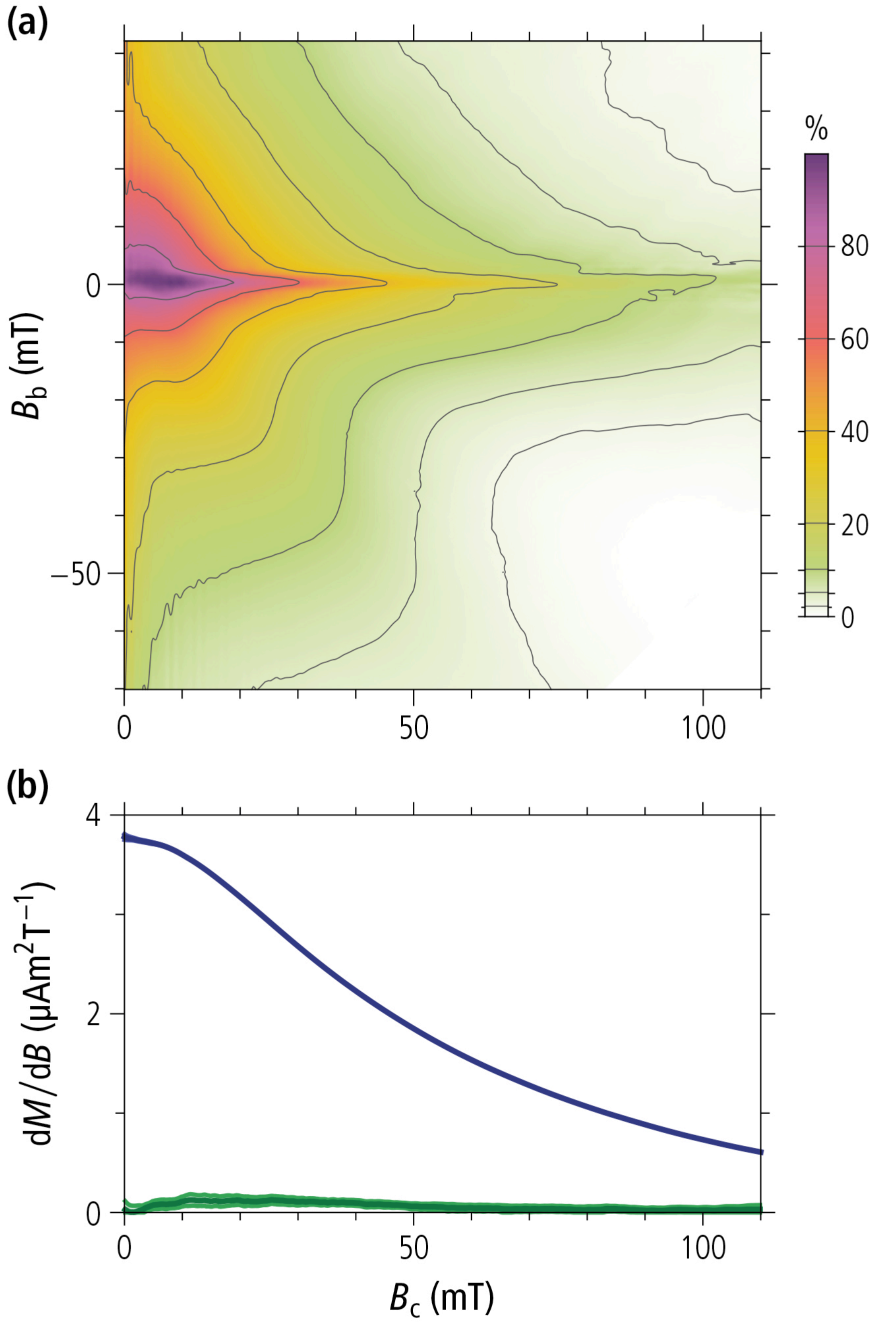

Figure S1: (a) FORC diagram of sample 17927 obtained from high-resolution measurements. Notice the overall triangular contour lines typical of PSD magnetite and the central ridge along $B_b = 0$, which signals the presence of a minor contribution from SD particles. (b) Coercivity distributions obtained from the subset of measurements corresponding to DC demagnetization (blue curve), and from the central ridge (green curve). Both curves are plotted with their 2σ confidence intervals.